Peer-reviewed version available at *Metabolites* **2019**, *10*, 14; doi:10.3390/metabo10010014

Article

13C-Metabolic Flux Analysis in Developing Flaxseed Embryos to Understand Storage Lipid Biosynthesis

Sébastien Acket [1]*, Anthony Degournay [1], Yannick Rossez [1], Stéphane Mottelet [2], Pierre Villon [3], Adrian Troncoso-Ponce [1], and Brigitte Thomasset [1]

[1] Alliance Sorbonne Université, Génie Enzymatique et Cellulaire, UMR CNRS 7025, Université de Technologie de Compiègne, 60205 Compiègne Cedex, France ; sebastien.acket@utc.fr (S.A.); anthony.degournay@utc.fr (A.D.); yannick.rossez@utc.fr (Y.R.); adrian.troncoso-ponce@utc.fr (A.T-P.); brigitte.thomasset@utc.fr (B.T.).

[2] Alliance Sorbonne Université, EA 4297 TIMR, Transformations Intégrées de la Matière Renouvelable, Université de Technologie de Compiègne, 60205 Compiègne Cedex, France; stephane.mottelet@utc.fr (S.M.).

[3] Alliance Sorbonne Université, Laboratoire Roberval, FRE UTC CNRS 2012, Université de Technologie de Compiègne, 60205 Compiègne Cedex, France; pierre.villon@utc.fr (P.V.).

* Correspondence: sebastien.acket@utc.fr;

Abstract: Flaxseed (*Linum usitatissinum L.*) oil is an important source of α-linolenic (C18:3 ω-3), this polyunsaturated fatty acid is well known for its nutritional role in human and animal diet. Understanding storage lipid biosynthesis in developing flaxseed embryos can lead to an increase in seed yield. While a tremendous amount of work has been done on different plant species to highlight their metabolism during embryos development, flaxseed metabolic flux analysis is still lacking. In this context, we have developed an in vitro cultured developing embryos of flaxseed and determined net fluxes by performing three complementary parallel labeling experiments with 13C-labeled glucose and glutamine. Metabolic fluxes were estimated by computer- aided modeling of the central metabolic network including 11 cofactors of 118 reactions of the central metabolism, 12 pseudo fluxes. A focus on lipid storage biosynthesis and the associated pathways was done in comparison with rapeseed, arabidopsis, maize and sunflower embryos. In our conditions, glucose was the main source of carbone of flaxseed embryos, leading to the conversion of phosphoenolpyruvate to pyruvate. The oxidative pentose phosphate pathway (OPPP) was identified as the producer of NADPH for fatty acid biosynthesis. Overall, the use of 13C-metabolic flux analysis provided new insight into flaxseed embryos metabolic processes involved in storage lipids biosynthesis. The elucidation of the metabolic network of this important crop plant reinforces the relevance of the application of this technique to the analysis of complex plant metabolic systems.

Keywords: parallel labeling experiments; metabolic flux analysis; flaxseed

1. Introduction

During the last decades the production and consumption of plant oil-derived products has steadily increased worldwide at about 5% per year [1]. It represents a current market value of over US$120 billion and its consumption is expected to almost double by 2030 [2]. This phenomenon is explained by factors ranging from the exponential growth of world population and its concomitant increase in food demand to the use of vegetal oils as feedstock for biodiesel production and other industrial products [3-4]. Four crops mainly fulfill this global demand: oil palm, soybean, rapeseed and sunflower [4-5]. The oil (TAG, triacylglycerols) produced by these plants is store in different tissues. These oils present qualitative differences in their composition: palmitic acid (16:0), a saturated

fatty acid, is the major fatty acid in palm oil, on the contrary, unsaturated fatty acids are well represented in the three other plant species oilseeds, e.g., oleic (18:1) and linoleic (18:2) acids [6-7]. The consumption of these different oils has repercussions on human health [8-9]. This is particularly important is the proportion of the essential fatty acids, linoleic (C18:2 ω-6) and α-linolenic (C18:3 ω-3), both precursors of long-chain polyunsaturated fatty acids (VLCPUFA), which are critical for maintaining a healthy physiological condition [8-9]. The ratio ω-6/ω-3 plays a fundamental role on human health. The optimal relationship between both unsaturated fatty acids has been identified around 4 to 1. However, this ratio is higher in current western diets (10:1 to 25:1), therefore, increasing ω-3 intakes will improve this balance [10]. Flaxseed oil is an important source of ω-3 fatty acids, α-linolenic acid is up more than 60% and the oil represents up to 43% of their seed weight [11-12]. In order to select cultivars richer in ω-3 fatty acids, understanding the carbon sources and metabolic fluxes leading to the synthesis and accumulation of these molecules is a critical step [13-14].

Fatty acid synthesis takes place in the plastids of developing seeds. This process relies on the photosynthetically assimilated carbon that is subsequently exported to the seeds in the form of sucrose [15-17]. Within the embryo, sucrose is enzymatically hydrolyzed, the resulting hexoses and hexoses-phosphates enter the glycolytic and the oxidative-pentose pathways to generate acetyl-CoA and reducing equivalents, to produce energy for de novo intraplastidial fatty acid synthesis. Glycolysis is compartmentalized within the cytosol and plastids but both metabolic routes communicate with each other by membrane transporters [17-19]. Acetyl-CoA must be synthetized within plastids because no transport to cross the plastidial membrane could be demonstrated, therefore its glycolytic precursors are generated within plastids or imported from the cytosol through the action of dedicated transporters [20]. Because of this dual location, the predominant source of carbon for plastidial acetyl-CoA is originated by one of the two glycolytic pathways. Although different approaches on diverse plants and tissues have been carried out in order to identify the main route from sucrose to fatty acids [21-23], the complexity of the process and the technical limitations of the methods used make this task difficult. Recently, the importance of the plastidial route during the fatty acid synthesis in Arabidopsis thaliana has been described [24].

In the present study, we have identified the major route of intracellular carbon with 13C metabolic flux analysis (13C-MFA) on developing flaxseed embryos. We have obtained the metabolic map by using complementary parallel labeling experiments. The main source of carbon for plastidial fatty acid synthesis in flaxseed embryos is discussed based on 13C-MFA studies in other vegetal species [25-31]. Therefore, the recognition of similarities and differences between diverse oilseeds shed light on the participation of the different carbon fluxes, from sucrose to fatty acids, during the active period of biosynthesis and accumulation of storage lipid in developing oilseeds.

2. Results

2.1. Optimal growth conditions

In order to characterize the synthesis of lipids in flaxseeds and identify the main contributing tissue (embryo or endosperm/seed coat), lipid accumulation during seed development was studied (Figure 1). Capsules were harvested from 14 to 50 DAF (days after flowering), flash freezed in liquid nitrogen and lyophilized. Total lipid content was determined following the protocol described by Bénard et al. (2018) [32]. Lipid content in flaxseed showed significant differences from 14 to 32 DAF (p-value < 0.05) (Figure 1a).

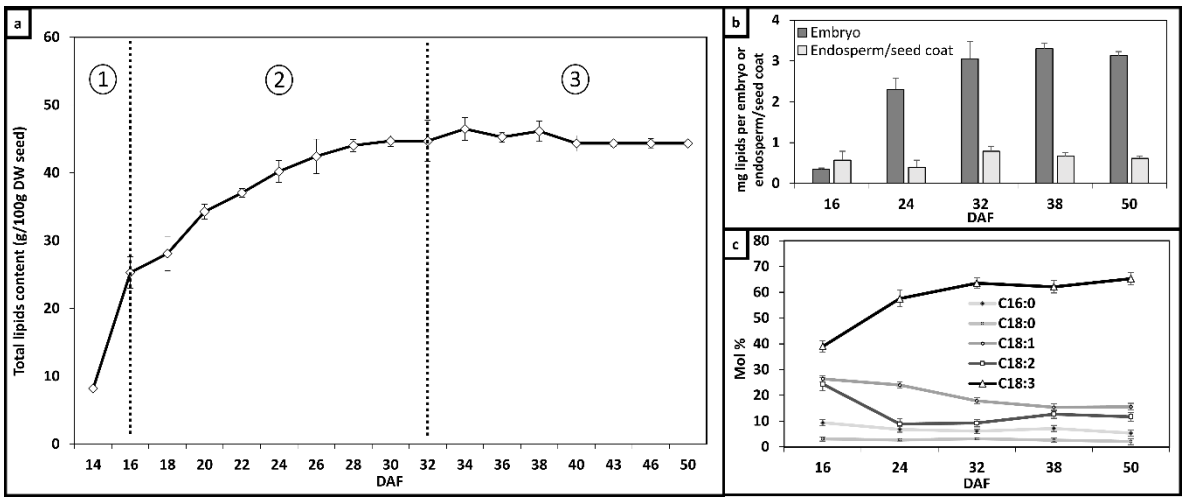

Figure 1. Synthesis of lipids and fatty acids in flaxseeds embryo and endosperm/seed coat during seed maturation. (a) Total lipids content in flaxseed expressed in g/100g DW; (b) Evolution of total lipids per tissue (mg lipids per embryo or endosperm/seed coat); (c) Relative fatty acids abundance in embryos during lipids accumulation (mol %). Data is represented as mean and variation (n = 4).

Based on linear velocities of lipid accumulation, three different periods were identified during flaxseed development. At 14-16 DAF (first stage), the lipid synthesis rate is 0.1 mg d-1 per seed (R2 = 0.99) corresponding to the beginning of lipid synthesis. Between 16-32 DAF (second stage) the highest rate of fatty acid synthesis is attained, with a value of 0.2 mg d-1 per seed (R2 = 0.97). After 32 DAF (third stage), the oil synthesis rate remained stable (0 mg d-1 per seed, R2 = 0.99). Lipid synthesis within embryos (Figure 1b) and endosperm/seed coat obtained from dissected seeds was characterized. In flaxseed, the endosperm is a thin layer of cell attached to the internal seed coat. The seed coat and endosperm are indistinguishable. Embryos showed a higher content and rate of synthesis, measured from 16 to 32 DAF, than endosperm/seed coat: 3.05 mg/embryo and 0.17 mg/d per tissue (R2 = 0.99) in the former tissue and 0.62 mg of endosperm/seed coat and 0.01 mg/d per tissue (R2 = 0.99) in the latter one. The fatty acid profile of embryos at 16, 24, 32, 38, and 50 DAF were analyzed by GC-MS (Figure 1c). A total of 5 fatty acids, C16:0, C18:0, C18:1, C18:2, and C18:3 were found in flax embryos. During the middle phase, C18:3 content increases in conjunction with a reduction of C18:2, from 39.9 to 63.5 and from 24.4 to 9.3 mol% respectively, while low levels of C18:0 and C16:0 remain stable. At 50 DAF, oil accumulated in the embryos is made up of C16:0 (5.3 mol%), C18:0 (2.1 mol%), C18:1 (15.6 mol%), C18:2 (11.7 mol%), and C18:3 (65.3 mol%).

2.2. *In vitro* culture of flaxseed embryos

Flaxseeds harvested at 16 DAF were dissected and their embryos sterilized and incubated during 24, 72, 120, and 168 hours with 16 ml of culture medium containing unlabeled substrates (culture A). For each time point, 4 independent cultures were made, and next embryos were placed in liquid nitrogen and lyophilized. In parallel, embryos extracted from 16, 17, 19, 21, and 23 DAF seeds, corresponding to 16 DAF and 24, 72, 120, and 168 hours respectively, were collected, placed in liquid nitrogen and lyophilized. In both cases, in vitro and in planta embryos time courses of dry weight showed similar values, from 0.77 to 3.08 mg/DW and to 2.40 mg/DW respectively (Figure 2a).

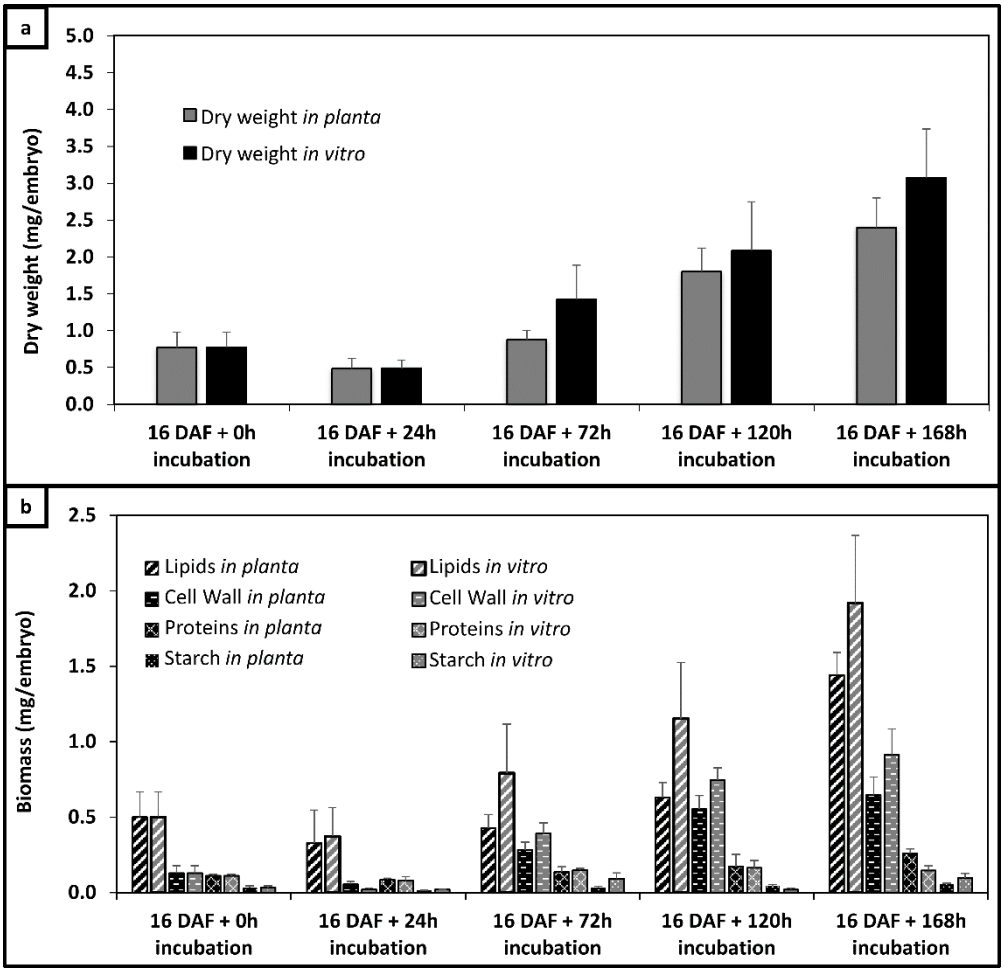

Figure 2. Weight and biomass composition between embryos cultured in vitro and its corresponding state in planta. (a) Dry weight between in planta vs in vitro expressed in mg/embryo; (b) Biomass accumulation between in vitro and in planta expressed in mg/embryo. Dry weight and biomass composition (lipids, proteins, cell wall and starch) content were determined as described in Material and Method section on flaxseed embryos cultivated from 16 DAF during 24, 72, 120 and 168h in culture medium A, containing unlabeled glucose and glutamine as carbon source. For each kinetic point, four independent experiments were made.

Biomass quantification was performed as described in references 25, 32, and 35. The main four components consituting 90% of the biomass are mainly, lipids (58% ± 2.1), soluble proteins (22% ± 1.2), cell walls (11% ± 1.3) and starch (5% ± 1.5) in planta. The composition in vitro and in planta during development was statistically similar and in both cases growth rate became linear upon 72 hours (Figure 2b). Together these results indicate that the culture conditions provide a good model for embryos metabolism in vitro. Concentrations of lipids, proteins, starch and cell wall were used for calculating both lower and upper bounds for external fluxes. External fluxes were calculated from the rate of growth of the embryos during their incubation and the biochemical composition of the reserve compounds because the proportion of embryo's biochemical components does not change during incubation. They correspond to the rate of accumulation of lipids (Vtag: 46.21 ± 5 mmol/gDW/d, proteins, Vprot: 105.59 ± 1.5 mmol/gDW/d cell wall, Vcw: 44.4 ± 2.30 mmol/gDW/d, and starch, Vsta: 1.0 ± 0.2 mmol/ gDW/d). The two main reaction in 13C-MFA models are the TAG and protein synthesis, these reactions drain the precursor metabolites and cofactors needed for cell expansion. To determine the coefficients in these reactions, biomass compositions were determined experimentally. Fatty acids composition was presented in Figure 1c while amino acid composition is presented in the Supplementary Table S1.

2.3. Metabolic and isotopic steady state

13C-based metabolic flux analysis performed at quasi-stationary steady state requires both metabolic and isotopic steady state conditions. Metabolic steady state is reached when the concentration of metabolic intermediates does not change while there is synthesis of reserve compounds [33]. In the model described in this manuscript, organic acids have been considered as metabolic intermediates and their concentrations have been measured within embryos (16 DAF) incubated at 24, 72, 120 and 168 hours in culture A. The concentrations of fumarate and succinate increase until reaching 0.45 and 1.15 µg/embryo respectively at 72 hours of incubation, meanwhile malate concentration rises to 4.55 µg/embryo at 120 hours of incubation (Figure 3). Upon 120 hours the concentration of these intermediates becomes stable ($p>0.05$).

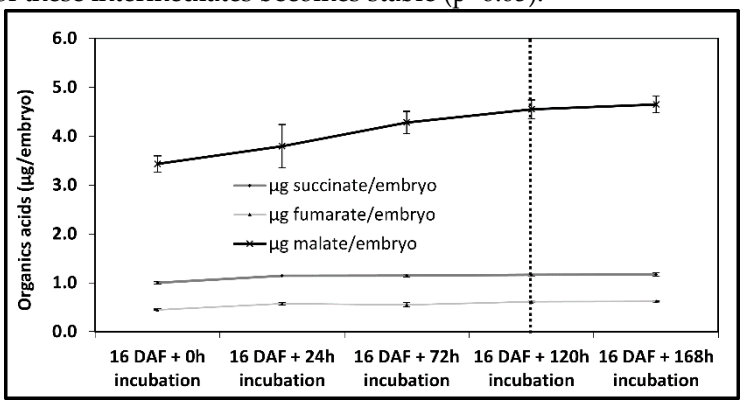

Figure 3. Concentration of organic acids (µg/embryo) during in vitro incubation. Organic acids concentrations were determined as described in Material and Method section on flaxseed embryos cultivated from 16 DAF during 24, 72, 120 and 168h in culture medium A, containing unlabeled glucose and glutamine as carbon source. For each kinetic point, four independent experiments were made.

With the aim of identifying the time required to reach the isotopic steady state condition, 16 DAF embryos were incubated with 16 ml of 20 mM [U-13C6] glucose, 80 mM glucose unlabeled, 160 mg/l, [U-13C5] glutamine and 640 mg/l glutamine unlabeled (culture B). After incubation periods of 24, 72, 120 and 168 hours, 4 independent cultures for each experimental point were performed, embryos were placed in liquid nitrogen and lyophilized. The quantification of isotopic enrichments of metabolites extracted from lyophilized embryos was carried out following the protocols proposed in references 34, 35 and 36. A total of 24 molecules were analyzed including free sugars, amino acids, organic acids and fatty acids. Isotopic steady state of free sugars [34] and organic acids was obtained at 72 hours, meanwhile, free amino acids [35] and fatty acids required 120 hours of incubation (Supplementary Table S2), consequently, the conditions necessary for quasi-stationary steady state, metabolic and isotopic steady state, were reached upon 120 hours of incubation.

2.4. Metabolic model construction

The central carbon network model required for 13C-MFA calculations was constructed based on the metabolic information available from different sources, including proteomic studies [21-22], genome sequencing information [37], EST libraries [11, 38-39], and other data related to seed [23, 25-31]. The developed model takes into account the stoichiometry of the reactions and describes the central carbon metabolism in developing flaxseed embryos during the lipid accumulation with condition-specific growth stoichiometries based on the measured biomass compositions. The model relies on the breakdown and transformation of two extracellular sources of carbon nutriments, glucose and glutamine, therefore it considers two input fluxes (Vg and Va respectively). Similarly, the model also considers five external fluxes corresponding to the accumulation of the main components of the generated biomass during the maturation stage: starch (Vsta), cell walls (Vcw), CO2 output (VCO2), triglycerides (Vtag) and proteins (Vprot). These input and external fluxes have been determined experimentally. The model includes all central carbon pathways found in flaxseed

embryos, reactions cytosolic and plastidial glycolysis, pentose phosphate pathway, Krebs cycle, anaplerotic and malic reactions, amino acids, sugars, fatty acids synthesis, cofactors balance, uridine diphosphate kinase (Vnrj4), non-growth associated ATP maintenance (Vnrj5) and ATP synthase. Starch degradation reaction (Vamy1) and ribulose-1,5-bis-phosphate carboxylase reaction (Vrubisco) was included, although flaxseed embryos are heterotrophic during the maturation phase [40]. Cofactors (ATP, ADP, NADP, NADPH, AMP, NAD, NADH, UDP, UTP, FADH2, and FAD) play a paramount role during the synthesis of biomass components, therefore they have been considered as internal metabolites within the network. The metabolic network is constrained with the carbon balance, the redox and energy status. A total of 118 reactions of the central carbon metabolism and 12 pseudo fluxes corresponding to the fraction of TAG and starch, already present in the cell, were modelized. A schematic representation of the model is given in Supplementary Table S3 and the complete list of reactions and metabolites are listed respectively in the Supplementary Table S4 and Supplementary Table S5.

2.5. 13C Metabolic flux analysis

2.5.1. Source of carbon for fatty acids synthesis

13C-MFA allowed the quantification of metabolic fluxes during reserve lipid accumulation in flax embryos and INCA software package was used for the calculations [41]. The program integrated: i) the metabolic model (118 reactions and 12 pseudo fluxes), ii) the extracellular fluxes (substrate consumption and synthesis of storage products), and iii) the experimental measures of the isotopic enrichments. Metabolic fluxes have been obtained by minimizing the variance-weighted sum of squared residuals (SSR) between the experimentally measured and model predicted mass isotopologue distributions of 19 metabolites (free sugars, free organics acids, free amino acids, and plastid acetyl-coA), with the measured external rates of three complementary labeling experiments (Culture B, C, D) to the metabolic model. The three labeling experiments are culture B (containing a mix of glucose and glutamine 13C), culture C (containing unlabeled glucose and glutamine 13C,) and culture D (containing glucose 13C and unlabeled glutamine). Thanks to the utilization of three parallel labeling experiments, estimated flux values were accurate and hence a precise carbon metabolic flux map was achieved [42]. Statistically acceptable fits were obtained, the minimized SSR values were lower than the maximum statistically acceptable SSR values at 95% confidence level. Comparisons between predicted and measured data are presented in Figure 4. The experimentally measured and simulated intracellular metabolite isotopologue are listed in Supplementary Table S6. The distribution is close to a linear relationship with a high correlation coefficient indicating that the mathematical flux model is fitting with the experimentally observed data.

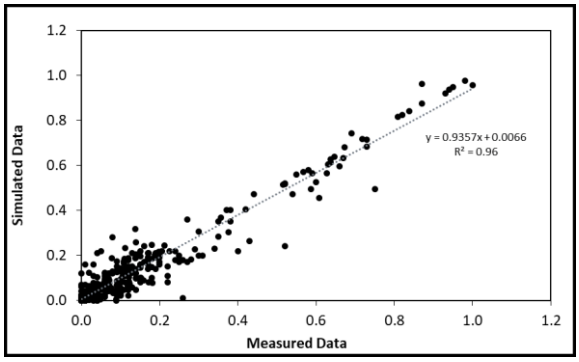

Figure 4. Comparison between predicted and measured data. The measured data correspond to the set of isotopologues of the three experimental conditions which made it possible to calculate the flux data (n = 53) at 95% confidence interval and represent four biological replicates per experimental condition. These data are presented in detail in the Supplementary Table S6. The linear regression equation and R2 value are shown.

Preprints (www.preprints.org) | NOT PEER-REVIEWED | Posted: 19 December 2019 doi:10.20944/preprints201912.0257.v1

Peer-reviewed version available at Metabolites 2019, 10, 14; doi:10.3390/metabo10010014

The complete set of best-fit flux values, including 95% confidence intervals for all fluxes are also provided in Supplementary Table S7. The 13C-MFA results point out that glucose is the main source of carbon for synthesis and accumulation of storage lipids (TAG) during flaxseed embryos development (Figure 5).

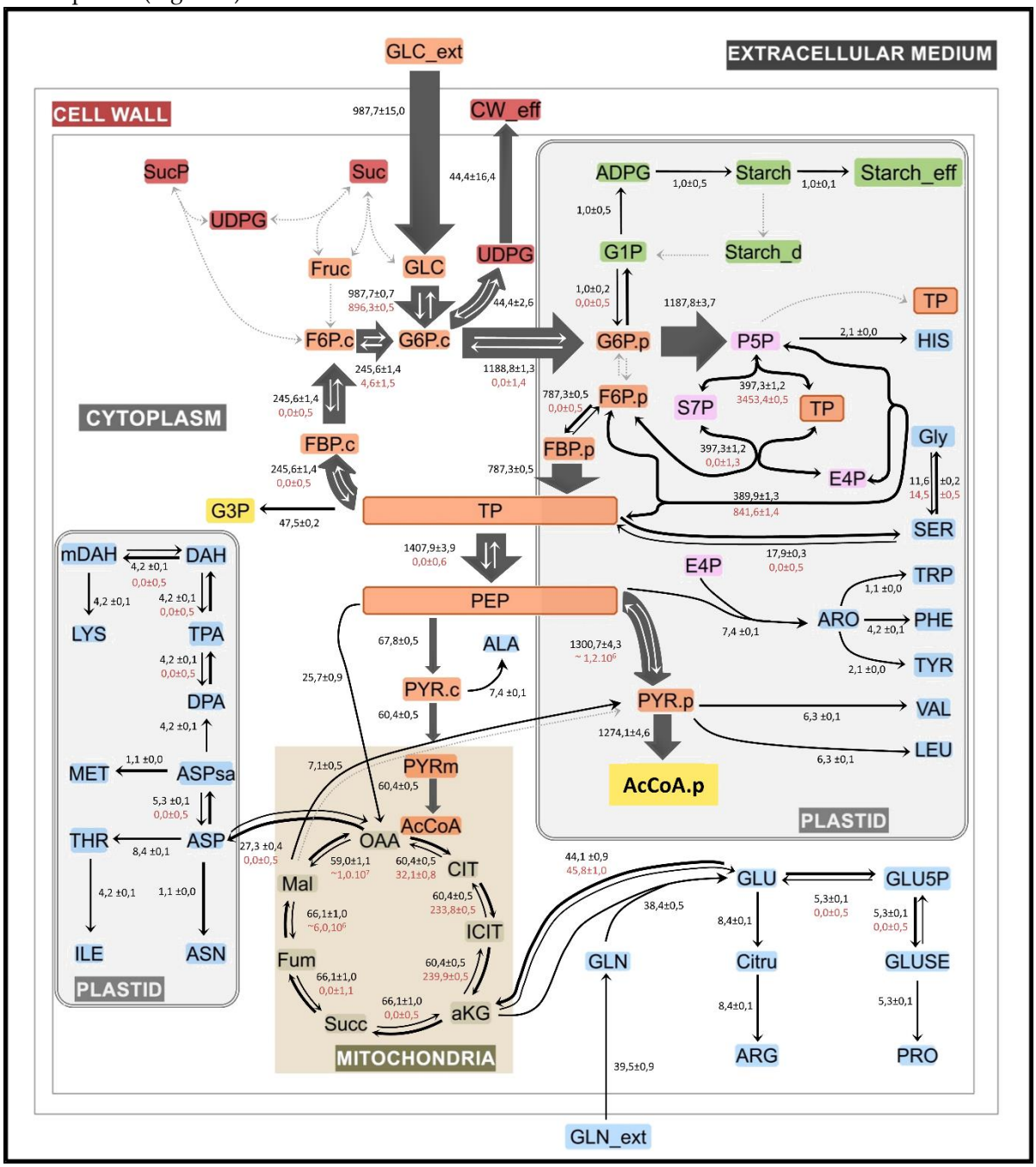

Figure 5. Metabolic network and fluxes in flaxseed embryos during maturation stage. The scheme presented is a simplified representation of the central carbon metabolism in flaxseed embryos during fatty acids synthesis and TAGs accumulation. Cytosolic and plastidial metabolites are specified by subscripts c and p, respectively, if the model distinguishes such subcellular species. All reactions, metabolites and abbreviations are available in Supplementary Table S4 and Supplementary Table S5. Values reported are the best fit obtained by INCA software using three parallel labeling experiments (53 metabolites and 6 extracellular fluxes). The average and standard deviation are calculated from four independent experiments. Fluxes are expressed in mmol/gDW/d ± confidence interval. The set of estimated fluxes values calculated by INCA software are presented in Supplementary Table S7. The metabolic map was drawn using the Omix software [43].

2.5.2. Source of cofactors for storage lipid biosynthesis

The formation of lipid has a high demands in the cofactors NADH and NADPH [44] and then these cofactors and others were measured (Supplementary Table S4). 1267 mmol NADPH/gDW/d, 1267 mmol NADH/gDW/d, 1267 mmol ATP/gDW/d were needed for fatty acid synthesis and 47.5 mmol NADH/gDW/d and 47.5 mmol ATP/gDW/d for the synthesis of G3P. Moreover, the model identified the oxidative pentose pathway reactions glucose-6-phosphate dehydrogenase and 6-phosphogluconate dehydrogenase (Vppp) as the main sources of NADPH. These reactions generated 2374 mmol NADPH/gDW/d, 339 times higher than the NADPH produced by the malic enzyme NADP-dependant (Vmal2). NADPH generated 1.9 times the demands required for fatty acid synthesis hence part of this pool contributes to the synthesis of amino acids within plastids (valine (VAL), leucine (LEU), proline (PRO), tryptophan (TRP), phenylalanine (PHE), and isoleucine (ILE)) and in the cytosol (proline (PRO) and glutamate (GLU)).

Another important cofactor for the synthesis of fatty acids and G3P is the NADH. The proposed model estimated that 1407 mmol NADH/gDW/d are required for TAG synthesis. Several reactions from different metabolic pathways produce NADH, although, two of them are the main sources of this molecule, glyceraldehyde-3-phosphate dehydrogenase (Vgapdh: 1407 mmol NADH/gDW/d) and pyruvate dehydrogenase (Vpdhp: 1274 mmol NADH/gDW/d). Other reactions associated to the Krebs cycle and to the amino acid biosynthetic pathways produce 287 mmol NADH/gDW/d. In total, NADH produced by these reactions 2.1 times the necessities requested by the synthesis of fatty acids and TAG. NADH is also consumed by reactions generating ATP (Vnrj2). ATP contributes as well to the synthesis of amino acids, fatty acids and TAG.

The required amount of ATP needed for the synthesis of fatty acids and G3P determined by the model is 1.4 mmol ATP/gDW/d. The proposed model considers six different ATP-generating reactions within three metabolic routes, energy reactions (Vnrj2, Vnrj3), glycolysis reactions (Vgapdh, Vpyrkp, Vpkc), and succinate biosynthetic pathway (Vnrj2). The reactions of glycolysis (Vgapdh, Vpyrkp) and energy (Vnrj2) mainly produce ATP, respectively 1407, 1300, 1403 mmol ATP/gDW/d, whereas the reactions Vpkc (67.8 mmol ATP/gDW/d), Vkdh (66.1 mmol ATP/gDW/d) and Vnrj3 (66.1 mmol ATP/gDW/d) produce less. Global ATP production has been calculated in 4310 mmol ATP/gDW/d, 3 times higher than the consumption during fatty acid and G3P synthesis, therefore, this production justifies the participation of this molecule in an array of metabolic processes (Supplementary Table S7).

3. Discussion

Oil accumulated in flaxseed embryos is made up of around 65% of polyunsaturated ω-3 linolenic acid, making flaxseed an important source of ω-3 fatty acids. Considerable efforts have been made in order to shed light to determine the fate of carbon from central metabolism to de novo fatty acid synthesis in the embryos, with genome assembly [37], transcriptomics [11, 38-39] and proteomics [21, 22] approaches.

Pyruvate is the substrate of the pyruvate dehydrogenase complex that converts this glycolytic metabolite into plastidial acetyl-CoA. The acetyl-CoA carboxylase catalyses the first committed step in de novo fatty acid synthesis. Therefore, the identification of the main pathway contributing to the generation of the plastidial pyruvate pool is an important step toward a better understanding of the carbon flux from carbohydrates to lipids in flaxseed metabolism. In this current work, the application of the state-of-the-art methods in 13C-MFA using a set of three parallel labeling experiments allowed the precise determination of metabolic fluxes, identifying the main carbon routes leading to oils and the principal sources of cofactors required by this metabolic process. By analyzing 13C-MFA, we identified that glucose is a carbon source for fatty acid synthesis, unlike glutamine. Glucose imported from culture medium is converted to G6P in the cytosol, exported to plastids to feed the OPPP and enter into the plastidial glycolysis up to the formation of PYR.p. The synthesis of PYR.p can be carried out either from PEP by pyruvate kinase, or from malate by malic enzymes or by transporting PYR from the cytosol to the plastid. Like maize [27, 45], sunflower [28], rapeseed [29-30], and arabidopsis thaliana [31] embryos, PYR.p is mainly synthesized from PEP by pyruvate kinase in flaxseed

embryos. Although this route is predominant, it is nevertheless higher in flax embryos (99.5%), compared to rapeseed embryos (74%), Arabidopsis thaliana (73%), sunflower (93%) and maize (between 70% and 54%) (Table 1).

Table 1. Comparison of carbon source for PYR.p and NADPH between flaxseed, rapeseed, *A.thaliana*, sunflower and maize cultivated developing embryos during lipid biosynthesis and accumulation calculated from 13C-MFA analysis.

		Flaxseed embryos Astral	Rapeseed embryos Reston [26,29-30]	A.thaliana embryos ws, pkp, col, wri [31]	Sunflower embryos Ames 7576 [28]	Maïze embryos LH 59[29]	Maïze embryos Alex [45]
Carbon source for PYR.p (mol %)	PEP -> PYR.p	99.50%	74%	73 to 88 %	93%	70%	54%
	MAL -> PYR.p	0.50%	NC	2%	7%	30%	46%
	PYR.c -> PYR.p	NC	26%	10 to 25 %	NC	NC	NC
Source of NADPH relative to demands for fatty acids biosynthesis (mol %)	by OPPP	187%	38%	-	106%	76%	74%
	by malic enzyme	0.55%	NC	-	7%	30%	56%

In flaxseed, rapeseed and Arabidopsis thaliana, the malic enzymes are not very active and generate respectively 0.5%, 0% and 2% of the PYR.p carbons, contrary to sunflower (7%) and maize (30%-46%) (Table I). However, differences between flax and rapeseed/Arabidopsis thaliana models remain. In rapeseed and Arabidopsis thaliana embryos, PYR.p synthesis is also generated by imports of pyruvate from the cytosol to the plastid at 26% and 25%, respectively. In the case of flax, a pyruvate transporter from cytosol to plastid was not identified by transcriptomics [11] or by proteomics [21-22] analyzes and was therefore not considered in the model developed. This transporter was also not taken into account in sunflower [28] and maize embryos [27, 45] metabolic fluxes because of the lack of molecular evidence for such a carrier in plants [46].

The storage lipid biosynthesis requires a significant energy intake, which is often limiting. This is particularly the case for NADPH and ATP. For flaxseed, rapeseed, sunflower and maize, NADPH mainly comes from OPPP reactions and, to a less extent, from the malic enzyme NADP dependent. Relative to demands of fatty acids synthesis, NADPH produced by OPPP reactions in flax embryos is in excess (187%) as observed for sunflower models (106%), while rapeseed (38%) and maize models (74-76%) do not fully meet the demand. For maize and sunflower models, NADP from malic enzyme is up to 30% and meet the demand. For arabidopsis and rapeseed models, no data are available about NADPH needs.

ATP produced by TCA cycle activity via oxidative phosphorylation relative to biosynthetic demands is in excess for maize (200%) [27] and sunflower (> 100%) [28] models but only partially in the arabidopsis (60%) [31], rapeseed (22%) [26, 29-30] and flax (5%) models, indicating reduced TCA cycle activity in C3 metabolism. In the case of flax, rapeseed and Arabidopsis, ATP production is provided by glycolysis reactions (Vgapdh, Vpyrkp, Vpkc) to form a pool necessary for storage lipid biosynthesis. Moreover, in flaxseed, the energetic reaction allowed the conversion of the surplus of NADPH and the use of ADP. This makes it possible to release a pool of NADH and ATP ensuring the cell growth and the lipid storage biosynthesis. Finally, in this study, we have deciphered flaxseed metabolism during lipid storage biosynthesis. This new knowledge can be used in the future for metabolic engineering studies in order to identify novel biomarkers to enhance breeding of flaxseed and yield improvements.

4. Materials and Methods

4.1. Chemicals and solutions

[U-13C6] glucose, [2-13C1] glucose and [U-13C5] glutamine were purchased from Cambridge Isotope Laboratories. Standards, minerals, vitamins and other compounds were purchased from Sigma. Solvents for LC-HRMS were purchased from Biosolve BV. All media and stock solutions were sterilized by filtration.

4.2. Plant material

Flax plant (Linum usitatissimum L.) line Astral were kindly provided by Laboulet semence (Airaines, France). Flax plants were grown in a greenhouse by applying the recommendations described in ref [32]. Briefly, the cultivation of plants has been done in a growth chamber at 60% relative humidity with a photoperiod of 16/8h day/night cycle (20/16°C) and a light intensity of 400 µmol photon m-2s-1. Flowers were tagged as petals opened. Flaxseeds used for biochemical characterization were harvested at 14, 16, 18, 20, 22, 24, 26, 28, 30, 32, 34, 36, 38, 40, 43, 46, and 50 DAF and immediately frozen in liquid nitrogen, and stored at −80 °C. For embryos culture, capsules were harvested at 16 DAF, sterilized for 20 min in 50% (v/v) bleach and then rinsed for 20 min with autoclaved water, prior to embryos removal and desiccation.

4.3. In vitro embryo culture

10 flaxseed embryos (16 DAF) aseptically dissected were transferred in a Petri dish containing 16 ml of an optimized culture medium. The culture medium reflects the composition of the embryo sac fluid [34-35]. It contained glucose (100 mM) and glutamine (800 mg/l) as macronutriments. It also included vitamins, mineral and micronutriments, KNO3 (125 mg/l), MgSO4.7H20 (370 mg/l), KCl (125 mg/l), KH2PO4 (10 mg/l), H3BO3 (10 mg/l), ZnSO4.7H20 (10 mg/l), Na2MoO4 (0.25 mg/l), CuSO4 (0.025 mg/l), CoCl2 (0.025), nicotinic acid (5 mg/l). The pH was maintained at 8.0 and 20% (w/v) polyethylene 4000 provided the osmoticum. 4 different cultures were made: one (A) containing unlabeled glucose and glutamine; a second (B) containing 20 mM [U-13C6] glucose and 160 mg/l [U-13C5] glutamine; a third (C) containing unlabeled glucose and 800 mg/l [U-13C5] glutamine, a fourth (D) containing 60 mM [U-13C6] glucose with 40 mM [2-13C1] glucose and unlabeled glutamine. Cultures A and B were performed during 24h, 72h, 120h, 168h, while culture C and D were performed at 168h of incubation. Four Petri dishes per point of kinetics and cultures were made for optimal results. Cultures were performed in a growth chamber at 18°C under a light intensity of 20 µE m-2 s-1, with a humidity of 60%. Culture A was carried out to: i: follow the evolution of the growth of embryos in vitro vs in planta; ii: determine the stationary metabolic state; iii: determine the rates of consumption of the substrates (glucose and glutamine), and accumulation rates of the compounds of reserves (lipids, proteins, cell wall and starch). Culture B was performed to determine the optimal incubation time for the stationary isotopic state to be reached necessary for 13C-MFA in stationary condition. The isotopic enrichments of the various metabolites from stationary isotopic B, C, D cultures were used as complementary parallel labeling experiments to determine the metabolic fluxes by simultaneous fit with the isotopic enrichments of all the metabolites of the 3 cultures with the mathematical model. For each culture, embryos were harvested and washed 3 times with 10 ml water to remove surface labeling. The embryos were then placed in liquid nitrogen and lyophilized to give the dry weight, biomass accumulation, isotopic enrichment of metabolites.

4.4. Biomass extraction and quantification

The methods used for extraction, separation and quantifying biomass composition were described in ref [27-28, 47]. For this, lipids, protein, starch and cell wall were extracted successively from 10 mg of lyophilized flaxseed embryos.

4.4.1. Lipids and fatty acids analysis

Lipids were extracted from flaxseeds and flaxseed embryos as described in ref [32]. Briefly, flaxseeds or flaxseed embryos were ground using a Precellys 24-Dual homogenizer during 5 minutes at 7.3 g in the presence of glass beads (0.5 mm) and 1 ml of hexane/isopropanol (2:1). After a centrifugation during 5 min at 16,000 g, the upper phase has been collected. The operation was repeated twice on the pellet to optimize lipids extraction. The three supernatants were then transferred to a previously weighed glass tube and the biomass pellet was dried at 40°C. Total lipid content was then determined gravimetrically after hexane evaporation under nitrogen. Lipids were derivatized by transesterification to generate Fatty Acid Methyl Esters (FAMEs) using Tetramethylammonium hydroxide (TMAH). For this, 5 mg of total lipid was resuspended in 100 µl of diethyl ether and were transesterified by addition of 5 µl of TMAH. The reaction was carried out at 25°C for 15 min with stirring at 625 rpm and then stopped by addition of 50 µl of decane. After centrifugation for 5 min at 16.1 g, 20 µl of the upper phase were taken and diluted in 178 µl of heptane to be analyzed by GC-MS.

FAMEs were analyzed using a ThermoFisher GC–MS (DSQ II) instrument equipped with a BPX70 capillary column (60 m x 0.25 mm; 0.25 µm) from SGE analytical science. FAMEs derivatives were separated by a gradient of temperature and using Helium as vector gas at a constant flow rate of 0.9 ml/min. The GC oven temperature was set at 140°C and held for 2 min. The oven temperature was then increased to 19°C/min to reach a final temperature of 230°C which was held for 2 min. The injection temperature was set at 230°C with a splitless mode. MS analysis was realized using electron impact (EI) ionization in positive ion mode. The ion source and interface temperatures were set at 230°C. Detection was in full scan 217 mode between m/z 50 and 500. GC-MS data were acquired and processed using Xcalibur software. FAMEs derivatives were identified using the NIST library and neat FAMEs standards purchased from Sigma.

4.4.2. Proteins and amino acids concentration

The dried pellet obtained in the previous step is taken up in 1 ml of 20 mM Tris-HCl extraction buffer, pH 7.5, 150 mM NaCl and 1% SDS as described in ref [27-28, 47]. After incubation during 15 min at 42°C in a shaker at 0.2 g the samples were centrifuged for 15 min at 16,000 g. The supernatant was recovered and the operation was repeated twice. The protein extract is then diluted to the tenth and 100 µl were then taken for protein quantification. Quantification of the soluble proteins present in our samples is based on the Lowry's method [48]. 125 µl of a solution of BIO-RAD copper tartrate alkaline buffer were added. After 10 min, 1 ml of Lowry's reagent was added, and the absorbance is read at 750 nm. Protein concentrations are determined using a standard range made with BSA (Bovine Serum Albumin) from 0 to 1.5 mg/ml. The pellet was dried again.

Extraction of the amino acids from the extracted soluble proteins is carried out by acid hydrolysis of the proteins. For this, the soluble proteins were first precipitated by adding 200 µl of trifluoroacetic acid. After 1.5 hours of incubation on ice, the samples were centrifuged for 20 min at 16,000 g and 250 µg/ml of [U-13C5] glutamine as internal standard was added to the supernatant. The pellet was taken up in 200 µl of HCl (6N). A 24h incubation at 110°C, 200 µl of 6N NaOH was added. After centrifugation for 10 min at 16,000g, the supernatants were recovered for injection into LC-HRMS. Quantification of the amino acids was performed using ultra high-pressure liquid chromatography (UPLC 1290 Infinity) coupled with high resolution–mass spectrometry (HRMS Q-TOF UHD 6538) from Agilent Technologies. The total LC-HRMS run was 30 min with a flow rate of 0.25 ml/min. Amino acids were separated on a Thermo Hypersyl Gold Phenyl (150 x 2.1 mm, 3 µm) at 20°C, using an elution gradient composed of a solution of 5 mM anhydrous pentafluoropropionic acid in water (solvent A) and acetonitrile (solvent B). The gradient was as follows: A = 0–4 min 99%, 4–12 min 12%, 12–15 min 70%, 15–30 min 2%. The mass spectra were acquired using a dual electrospray ionization in positive-ion mode. The source temperature, fragmentor and the skimmer were set up respectively at 350°C, 120 V, 65 V. The acquisition was made in full scan mode between 50 m/z and 1050 m/z, with a scan of two spectra per second. MassHunter B.07 software allowed to control the parameters of the machine, acquired and processed the data. Amino acid quantification was performed by injection of amino acid

standards between 20 µg/ml to 500 µg/ml contained 250 µg/ml of [U-13C5] glutamine as internal standard.

4.4.3. Starch and cell wall

Extraction and quantification of the starch is achieved using a Total Starch Assay Kit (AA/AMG) from Megazyme International Ireland Ltd Starch. Extraction was performed on the pellets after protein extraction. The remaining metabolites, minerals and vitamins were removed by washing the pellets 3 times with water and 3 times with ethanol. Samples are taken up in 1 ml of water, stirred for 5 min in a shaker at 2.3 g and the supernatant was removed. This washing is done three times with water and three times with ethanol. The pellet obtained is taken up in 600 µl of a solution of α-amylase with 250 µg/ml of [U-13C6] glucose as internal standards, (sodium acetate pH 4.8, α-amylase 1600 U/ml (30/1), (v/v)) and incubated at 100°C during 30 min. Once the mixture has cooled down to room temperature, 20 µl of α-amyloglucosidase (200 µM) were added, and samples were incubated during 30 min at 50°C. After centrifugation (5 min at 16,000 g), a 500 µl aliquot of supernatant was pipetted into a 1.5 ml tube to be used for quantification by LC-HRMS. Separation condition were performed as previously described in ref [34]. Quantification was performed by injecting glucose standards between 20 µM to 500 µM containing 250 µg/ml of [U-13C6] glucose as internal standard. Total cell wall content was then determined gravimetrically after the pellet was successively washed (three times with water, three times with 70% ethanol and three times with acetone) and dried 72h under the fumehood as described in ref [27-28, 47].

4.5. Metabolites extraction

Water-soluble metabolites (free sugars, free amino acids, and organic acid) were extracted from 10 mg of dried flaxseed embryos as described in ref [36]. Briefly, after extracting lipids as described previously, the pellet is taken up in 1 ml of boiling 0.01% HCl and placed in a water bath at 95°C for 15 min. After centrifugation for 10 min at 16,000 g, the supernatants were filtered (0.22 µm) and collected. This procedure was repeated 3 times, to maximize metabolite extraction. Supernatants were frozen, freeze-dried and taken up in 1 ml of sodium acetate buffer (50 mM, pH 5.5). Samples were loaded onto a cation exchange resin (Dowex 50×8 [Hydrogen form, 200–400]) to collected free amino acids fractions. The recovered fraction containing the free sugars and organic acids were loaded onto an anion exchange resin (Dowex 1x8 [formate form, 200–400, Supelco 13858]). Free sugars were collected after an elution with 5 ml of water whereas organic acids were eluted using formic acid (4 M). The three fractions (amino acids, organic acids, free sugars) were frozen and lyophilized to be taken up in 500 µl of water for the determination of the isotopic enrichment of these molecules.

4.6. Isotopic enrichment of metabolites

Isotopic enrichments were determined on FAMEs, and water-soluble metabolites (free sugars, free amino acids, and organic acid). FAMEs have been separated and analyzed as previously described. Labeling of FAMEs was determined on the base peak of methyl palmitate. This peak corresponds to the McLafferty rearrangement fragment (m/z 74). It has two carbons from plastidial acetyl CoA (AcCoA.p). Labeling of free sugars and free amino acids were determined as described in ref [34-35,49].

Organic acids were separated using ultra high-pressure liquid chromatography (UPLC 1290 Infinity) coupled with high resolution–mass spectrometry (HRMS Q-TOF UHD 6538) from Agilent Technologies. Organic acids were separated on a Dionex Acclaim OA column (150 x 2.1 mm, 3 µm), at a flow rate of 0.5 ml/min with isocratic condition (0.2% formic acid in water). The total LC-HRMS run was 5 min. At the end of the chromatographic column, the eluted molecules were identified by mass spectrometry. Organic acids were ionized in negative mode using a dual electrospray ionization at 350 °C with a fragment of 120 V and a value of 65 V Skimmer. Organic acids were detected in full scan mode using a mass range from 100 m/z to 3000 m/z. Organic acids were identified by finding the exact mass and retention time of the succinate, fumarate, citrate/isocitrate and malate standards. Mass

isotopologue distributions were obtained by integration of isotope mass from base peaks [M-H+], and corrected for natural abundances using Scilab.

4.7. Modeling metabolic pathways

A central carbon metabolic network model of flaxseed embryos was constructed for 13C-MFA analysis. The metabolic model described in Supplementary Table S3 was programmed in the INCA software [41], based on the elementary metabolite units decomposition to the underlying isotopologue network (EMU). Intracellular fluxes were estimated by the best fit of three complementary labeling experiments in parallel (mass isotopologue distributions of 53 intracellular metabolites and 6 extracellular fluxes measured of Cultures B, C and D) with model predicted to a single flux model. As initial program, 2000 different starting points (random initial values) by using a Levenberg-Marquardt optimization algorithm [50] were used. After fixing the best value, an optimization program was performed with 300 starting points. Accurate 95% confidence intervals were computed for all estimated fluxes by evaluating the sensitivity of the minimized SSR to flux variations. Least-squares parameter regression, statistical and sensitivity analysis of the optimal solution, was performed using the INCA software [41]. A $\chi 2$ statistical test to assess goodness of fit and accurate 95% confidence intervals were computed by evaluating the sensitivity of the minimized SSR to flux variations. Assuming that the model is correct when the acceptable range of SSR values is between 95% confidence interval [51]. According to [45], a linear regression of a comparison between mass isotopologue distribution measured and simulated (Figure 3 and Supplementary Table S6) with a coefficient of variation close to 1 allows to validate the model. The metabolic map was drawn using Omix Software [43]. The results are presented in Figure 4 and Supplementary Table S7.

Supplementary Materials: The following are available online, Figure S1: The metabolic network of flaxseed embryos cell, Table S1: The amino acid composition of proteins, Table S2: Evolution of the isotopic enrichment of free organic acids and two carbons from palmitic acid (C16:0) extracted from developing embryos harvested at 16DAF incubated during 24h, 72h, 120h, 168h in the culture medium B, containing 80mM unlabeled glucose, 20 mM [U-13C]glucose, 640mg/l unlabeled glutamine, 160mg/l [U-13C] glutamine, Table S3: Lists of reactions used with carbon transition of the metabolic network of flaxseed embryos cell, Table S4: Lists of metabolites and details of their abbreviations used in the metabolic network of flaxseed embryos cell., Table S5: Comparison between mass isotopomer distribution measured and simulated, Table S6: Metabolic fluxes in flaxseed embryos during lipids accumulation.

Author Contributions: Conceptualization, S.A., B.T.; methodology, S.A.; software, S.M.; S.A.; formal analysis, S.A.; investigation, S.A.; data curation, S.A., S.M., B.T.; writing—original draft preparation, S.A., A.T.-P., Y.R.; writing—review and editing, A.T.-P., Y.R., B.T.; visualization, S.A., A.D.; supervision, B.T.; P.V.; project administration, B.T.; funding acquisition, P.V., B.T.

Funding: This research was funded by SAS PIVERT, within the frame of the French Institute for the Energy Transition (Institut pour la Transition Energétique (ITE) P.I.V.E.R.T (www.institut-pivert.com), supported, as part of the Investments for the Future ("Investissements d'Avenir"), by the French Government under the reference ANR-001-01. This study was funded by the Regional Council of Picardy and European Union co-founded equipments utilized within CPER 2007-2020. The authors would also like to thank the Hauts-de-France Region and the European Regional Development Fund (ERDF) 2014/2020 for the funding of this work.

Conflicts of Interest: The authors declare no conflict of interest.

References

1. Chen, G.; Woodfield, H.K; Pan, X.; Harwood, J.L.; Weselake, R.J. Acyl-trafficking during plant oil accumulation. *Lipids* **2015**, *50*, 1057–1068.
2. Troncoso-Ponce, MA.; Kilaru, A.; Cao, X., Durrett, TP.; Fan, J.; Jensen, JK.; Thrower, N.A.; Pauly, M.; Wilkerson, C.; Ohlrogge, J.B. Comparative deep transcriptional profiling of four developing oilseeds. *Plant J* **2011**, *68*, 1014-1027.
3. McKeon, T.A.; Hayes, D.G.; Hildebrand, D.F.; Weselake, R.J. Introduction to industrial oil crops, Industrial Oil Crops. *AOCS Press* **2016**, *1*, 1–13.

4. Zafar, S.; Li, Y.L.; Li, N.N.; Zhu, K.E.; Tan, X.L. Recent advances in enhancement of oil content in oilseed crops. *J.Biotechnol* **2019**, *10*, 35–44.
5. Dyer, J.M.; Mullen, R.T. Engineering plant oils as high-value industrial feedstocks for biorefining: the need for underpinning cell biology research. *Physiol. Plant* **2008**, *132*, 11–22.
6. Dubois, V.; Breton, S.; Linder, M.; Fanni, J.; Parmentier, M. Fatty acid profiles of 80 vegetable oils with regard to their nutritional potential. *Eur J Lipid Sci Technol* **2007**, *109*, 710–732.
7. Ohlrogge, J.; Thrower, N.; Mhaske, V.; Stymne, S.; Baxter, M.; Yang, W.; Liu, J.; Shaw, K.; Shorrosh, B.; Zhang, M.; Wilkerson, C.; Matthäus, B. PlantFAdb: a resource for exploring hundreds of plant fatty acid structures synthesized by thousands of plants and their phylogenetic relationships, *Plant J* **2018**, *96*, 1299–1308.
8. Orsavova, J.; Misurcova, L.; Ambrozova, J.V.; Vicha, R.; Mlcek, J. Fatty acids composition of vegetable oils and its contribution to dietary energy intake and dependence of cardiovascular mortality on dietary intake of fatty acids. *Int J Mol Sci* **2015**, *16*, 12871–12890.
9. Spencer, S.J.; Koroi, A.; Layé, S.; Shukitt-Hale, B.; Barrientos, R.M. Food for thought: how nutrition impacts cognition and emotion. *NPJ Sci Food* **2017**, *6*, 1–7.
10. Jhala, J.A.; Hall, M.L. Flax (Linum usitatissimum L.): Current Uses and Future Applications. *Australian J. Basic Appl. Sci* **2010**, *4*, 4304–4312.
11. Venglat, P.; Xiang, D.; Qiu, Q.; Stone, L.S.; Tibiche, C.; Cram, D.; Alting-Mees, M.; Nowak, J.; Cloutier, S.; Deyholos, M.; Bekkaoui, F.; Sharpe, A.; Wang, E.; Rowland, G.; Selvaraj, G.; Dalta, R. Gene expression analysis of flax seed development. *BMC Plant Biology* **2011**, *11*, 11-17.
12. Basch, E.; Mphil, D.; Bent, S.; Collins, J.; Dacey, C.; Hammerness, P.; Harrisson, M.; Smith, M.; Szapary, P.; Ulbritcht, C.; Vora, M.; Weissner, W. Flax and flaxseed oil (Linum usitatissimum): a review by the Natural Standard Research Collaboration. *J. Soc. Int. Onc* **2007**, *5*, 92–105.
13. Pollard, M.; Martin, T.M.; Shachar-Hill, Y. Lipid analysis of developing Camelina sativa seeds and cultured embryos. *Phytochemistry*, **2015**, *118*, 23–32.
14. Ramli, U.S.; Salas, J.J.; Quant, P.A.; Harwood, J.L. Use of metabolic control analysis to give quantitative information on control of lipid biosynthesis in the important oil crop, Elaeis guineensis (oilpalm). *New Phytol* **2009**, *184*, 330–339.
15. Stadler, R.; Lauterbach, C.; Sauer, N. Cell-to-cell movement of green fluorescent protein reveals post-phloem transport in the outer integument and identifies symplastic domains in Arabidopsis seeds and embryos. *Plant Physiol* **2005**, *139*, 701–712.
16. Yadav, U.P.; Ayre, B.G.; Bush, D.R. Transgenic approaches to altering carbon and nitrogen partitioning in whole plants: assessing the potential to improve crop yields and nutritional quality. *Front. Plant Sci* **2005**, *6*, 1-13.
17. Lemoine, R.; La Camera, S.; Atanassova, R.; Dédaldéchamp, F.; Allario, T.; Pourtau, N.; Bonnemain, J.L.; Laloi, M.; Coutos-Thévenot, P.; Maurousset, L.; Faucher, M.; Girousse, C.; Lemonnier, P.; Parrilla, J.; Durand, M. Source-to-sink transport of sugar and regulation by environmental factors. Front. *Plant Sci* **2013**, *4*, 1-21.
18. Baud, S.; Lepiniec, L. Physiological and developmental regulation of seed oil production. *Prog Lipid Res* **2010**, *49*, 235-249.
19. Baud, S.; Boutin, J.P.; Miquel, M.; Lepiniec, L.; Rochat, C. An integrated overview of seed development in Arabidopsis thaliana ecotype WS. *Plant Physiol Biochem* **2002**, *40*, 151-160.
20. Li-Beisson, Y.; Shorrosh, B.; Beisson, F.; Andersson, M.X.; Arondel, V.; Bates, P.D.; Baud, S.; Bird, D.; Debono, A.; Durrett, T.P.; Franke, R.B.; Graham, I.A.; Katayama, K.; Kelly, A. A.; Larson, T.; Markham, J.E.; Miquel, M.; Molina, I.; Nishida, I.; Rowland, O.; Samuels, L.; Schmid, K.M.; Wada, H.; Welti, R.; Xu, C.; Zallot, R.; Ohlrogge J.B. Acyl-lipid metabolism. In *Arabidopsis Book.*; The American Society of Plant Biologists.; Eds.; Rockville, USA, 2013; Volume 2013, pp. 1-65.
21. Barvkar, V.T.; Pardeshi, V.C.; Kale, S.M.; Kadoo, N.Y.; Giri, A.P.; Gupta, V.S. Proteome profiling of flax (Linum usitatissimum) seed: characterization of functional metabolic pathways operating during seed development. *J. Proteome Res* **2012**, *11*, 6264-7626.
22. Klubicová, K.; Danchenko, M.; Skultety, L.; Berezhna, V.V.; Rashydov, N.M.; Hajduch, M. Radioactive Chernobyl environment has produced high-oil flax seeds that show proteome alterations related to carbon metabolism during seed development. *J. Proteome Res* **2013**, *12*, 4799- 4806.

23. Schwender, J.; Ohlrogge, J.B. Probing in vivo metabolism by stable isotope labeling of storage lipids and proteins in developing Brassica napus embryos. *Plant Physio* **2002**, *130*, 347–361.
24. Flores-Tornero, M.; Anoman, A.D.; Rosa-Tellez, S.; Toujani, W.; Weber, A.P.; Eisenhut, M.; Kurz, S.; Alseekh, S.; Fernie, A.R.; Munoz-Bertomeu, J.; Ros, R. Overexpression of the triose phosphate translocator (TPT) complements the abnormal metabolism and development of plastidial glycolytic glyceraldehyde-3-phosphate dehydrogenase mutants. *Plant J* **2017**, *89*, 1146-1158.
25. Schwender, J.; Ohlrogge, J.B. Probing in vivo metabolism by stable isotope labeling of storage lipids and proteins in developing Brassica napus embryos. *Plant Physio* **2002**, *130*, 347–361.
26. Schwender, J.; Ohlrogge, J.B.; Shachar-Hill, Y. A flux model of glycolysis and the oxidative pentosephosphate pathway in developing Brassica napus embryos. *J. Biol. Chem* **2003**, *278*, 29442–29453.
27. Alonso, A.P.; Dale, V.L.; Shachar-Hill, Y. Understanding fatty acid synthesis in developing maize embryos using metabolic flux analysis. *Metabolic Engineering* **2010**, *12*, 488–497.
28. Alonso, A.P.; Goffman, F.D.; Ohlrogge, J.B.; Shachar-Hill, Y. Carbon conversion efficiency and central metabolic fluxes in developing sunflower (Helianthus annuus L.) embryos. *Plant J* **2007**, *52*, 296–308.
29. Schwender, J.; Goffman, F.; Ohlrogge, J.B.; Shachar-Hill, Y. Rubisco without the Calvin cycle improves the carbon efficiency of developing green seeds. *Nature* **2004**, *432*, 779–782.
30. Schwender, J.; Shachar-Hill, Y.; Ohlrogge, J.B. Mitochondrial metabolism in developing embryos of Brassica napus. *Journal of Biological Chemistry* **2006**, *281*, 34040–34047.
31. Lonien, J.; Schwender, J. Analysis of metabolic flux phenotypes for two Arabidopsis mutants with severe impairment in seed storage lipid synthesis. *Plant Physio*. **2009**, *151*, 1617–1634.
32. Benard, C.; Acket, S.; Rossez, Y.; Fernandez, O.; Berton, T.; Gibon, Y.; Cabasson, C. Untargeted analysis of semipolar compounds by LC-MS and targeted analysis of fatty acids by GC-MS/GC-FID: From plant cultivation to extract preparation. In: *Plant Metabolomics*, Antonio, C. ed.; Method in Molecular Biology, Eds.; Humana Press, New York, USA; Volume 1778, pp. 101-124.
33. Jazmin L.J., O'Grady J.P., Ma F., Allen D.K., Morgan J.A., Young J.D. Isotopically Nonstationary MFA (INST-MFA) of Autotrophic Metabolism. In: *Plant metabolic flux analysis*, Dieuaide-Noubhani, M., Alonso, A.; Eds.; Humana Press, Totowa, USA; Volume 1090, pp. 181-210.
34. Acket, S.; Degournay, A.; Merlier, F.; Thomasset, B. 13C labeling analysis of sugars by high resolution-mass spectrometry for Metabolic Flux Analysis. *Anal. Biochem* **2017**, *527*, 45-48.
35. Acket, S.; Degournay, A.; Gosset, M.; Merlier, F.; Troncoso-Ponce, MA.; Thomasset, B. Analysis of 13C labeling amino acids by capillary electrophoresis - High resolution mass spectrometry in developing flaxseed. *Anal. Biochem* **2018**, *547*, 14-18.
36. Koubaa, M.; Cocuron, J. C.; Thomasset, B.; Alonso, A. P. Highlighting the tricarboxylic acid cycle: liquid and gas chromatography-mass spectrometry analyses of 13C-labeled organic acids. *Anal Biochem* **2013**, *436*, 151-159.
37. Wang, Z.; Hobson, N.; Galindo, L.; Zhu, S.; Shi, D.; McDill, J.; Yang, L.; Hawkins, S.; Neutelings, G.; Datla, R.; Lambert, G.; Galbraith, D.W.; Grassa, C.J.; Geraldes, A.; Cronk, Q.C.; Cullis, C.; Dash, P.K.; Kumar, P.A.; Cloutier, S.; Sharpe, A.G.; Wong, G.K.S.; Wang, J.; Deyholos, M.K. The genome of flax (Linum usitatissimum) assembled de novo from short shotgun sequence reads. *Plant J* **2012**, *72*, 461– 473.
38. Fenart, S.; Assoumou Ndong, Y-P.; Duarte, J.; Rivière, N.; Wilmer, J.; Van Wuytswinkel, O.; Lucau, A.; Cariou, E.; Neutelings, G.; Gutierrez, L.; Chabbert, B.; Guillot, X.; Tavernier, R.; Hawkins, S.; Thomasset, B. Development and validation of a flax (Linum usitatissimum L.) gene expression oligo microarray. *BMC Genomics* **2010**, *11*, 1-14.
39. Fenart, S.; Chabi, M.; Gallina, S.; Huis, R.; Neutelings, G.; Riviere, N.; Thomasset, B.; Hawkins, S.; Lucau-Danila, A. Intra-platform comparison of 25-mer and 60-mer oligonucleotide Nimblegen DNA microarrays. *BMC Research Notes* **2013**, *6*, 1-11.
40. Troufflard, S. Study of carbon metabolism in linseed developing embryos during lipid storage accumulation. Thèse de l'Université de Picardie Jules Verne, Amiens, France, **2004**, http://www.theses.fr/2004AMIE0419.
41. Young, JD. INCA: A computational platform for isotopically non-stationary metabolic flux analysis. *Bioinformatics* **2014**, *30*, 1333–1335.
42. Leighty, RW.; Antoniewicz, MR. COMPLETE-MFA: complementary parallel labeling experiments technique for metabolic flux analysis. *Metab Eng* **2013**, *20*, 49–55.

43. Droste, P.; Nöh, K.; Wiechert, W. Omix – A visualization tool for metabolic networks with highest usability and customizability in focus. *Chemie Ingenieur Technik* **2013**, *85*, 849–862.
44. Schwender, J.; Hay, J.O. Predictive modeling of biomass component tradeoffs in Brassica napus developing oilseeds based on in silico manipulation of storage metabolism. *Plant Physio* **2012**, *160*, 1218-1236.
45. Cocuron, J.C.; Koubaa, M.; Kimmelfield, R.; Ross, Z.; Alonso, A.P. A combined metabolomics and fluxomics analysis identifies steps limiting oil synthesis in maize embryos. *Plant Physio* **2019**, *181*, 961-975.
46. O'Grady, J.; Schwender, J.; Shachar-Hill, Y.; Morgan, J.A. Metabolic cartography: experimental quantification of metabolic fluxes from isotopic labeling studies. *J. Exp. Bot* **2012**, *63*, 2293–2308.
47. Goffman, F.D.; Alonso, A.P.; Schwender, J.; Shachar-Hill, Y.; Ohlrogge, J.B. Light enables a very high efficiency of carbon storage in developing embryos of rapeseed. *Plant Physio* **2005**, *138*, 2269–2279.
48. Lowry, O. H.; Rosenbrough, N. J.; Farr, A. L.; Randall, R. J. Protein measurement with the Folin phenol reagent. *J Biol Chem* **1951**, *193*, 265-275.
49. Acket, S.; Degournay, A.; Merlier, F.; Thomasset, B. Data documenting the comparison between the theoretically expected values of free sugars mass isotopomer composition with standards using GC-MS and LC-HRMS for Metabolic Flux Analysis. *Data in Brief* **2017**, *12*, 108-112.
50. Young, JD.; Walther, JL.; Antoniewicz, MR.; Yoo, H.; Stephanopoulos, G. An Elementary Metabolite Unit (EMU) based method of isotopically nonstationary flux analysis. *Biotechnol Bioeng* **2008**, *99*, 686–699.
51. Antoniewicz, MR.; Kelleher, JK.; Stephanopoulos, G. Determination of confidence intervals of metabolic fluxes estimated from stable isotope measurements. *Metab Eng* **2006**, *8*, 324–337.